

## Tuning Work Function of Noble Metals As Promising Cathodes in Organic Electronic Devices

Fenghong Li,\* Yi Zhou, Fengling Zhang, Xianjie Liu, Yiqiang Zhan, and Mats Fahlman

Department of Physics Chemistry and Biology, Linköping University, 581 83 Linköping, Sweden

Received February 19, 2009. Revised Manuscript Received May 5, 2009

Work function (WF) modification of metal electrodes by adsorbing electron-rich or electron-deficient molecules on metal surfaces has become a field of significant interest. The barrier for charge carrier injection in organic semiconductor devices can be reduced by molecular adsorption, leading to an interfacial dipole. Here, we demonstrate that the WF of noble metals such as Au can be decreased significantly by adsorbing air stable n-type dopant acridine orange base (AOB) thin film. When a (sub)monolayer AOB is deposited on sputter-cleaned Au, the WF of the substrate changes from 5.2 to 3.5 eV. At complete coverage of the Au surface, the WF is further reduced to 3.3 eV. When a (sub) monolayer of AOB is inserted between Au and C<sub>60</sub> thin film, the barrier of electron injection is decreased by 0.4 ± 0.1 eV as compared to an Au–C<sub>60</sub> interface without AOB. Polymer solar cells with AOB/Au as a cathode have a similar open circuit voltage and comparable power conversion efficiency with devices using LiF/Al as a cathode, demonstrating that the AOB-modified gold electrode is an efficient low-work-function contact. Given the low positive pinning energy of 3.3 eV for AOB, we expect that other conventional high-work-function materials (Ag, ITO, La<sub>0.7</sub>Sr<sub>0.3</sub>MnO<sub>3</sub> and even PEDOT:PSS) can be modified by AOB as effectively as Au.

### Introduction

Work function (WF) of electrodes significantly affects the performances of organic electronic devices. It is desirable to tune the WF of metal electrodes for matching LUMO or HOMO of organic molecules. Results from different groups have shown that the barrier of charge carrier injection in organic semiconductor devices can be tuned by molecular adsorption leading to an interfacial dipole.<sup>1–3</sup> An interfacial dipole with its negative pole pointing toward the organic molecule and its positive pole toward the metal increases the metal work function. As a result, the barrier for hole-injection is reduced. Reversing the direction of the interfacial dipole reduces the work function, improving electron injection. The mechanisms for dipole formation at organic molecule/metal interfaces can be grouped by the adsorbate interaction strength from weak to strong as follows: (1) noble gas atoms or saturated hydrocarbons on clean metals where the dipole is formed due to “push back effect” associated with Pauli repulsion;<sup>1,3</sup> (2) physisorption of molecules followed by integer charge transfer to the substrate;<sup>3</sup> (3) chemisorbed molecules that donate/accept charge to/from the substrate;<sup>1–4</sup> (4) covalently bonding molecules such as self-assembled monolayers (SAMs)

carrying an intrinsic net dipole moment.<sup>2,3,5</sup> Tetrakis (dimethylamino)ethylene (TDAE) is known as a strong electron donor, as demonstrated in the organic ferromagnetic compound TDAE–C<sub>60</sub>,<sup>6</sup> and the feasibility of using TDAE for work function modification of high work function air-stable substrates has been investigated extensively.<sup>7–10</sup> These studies show that electron transfer occurs from TDAE to the substrate at the interface, resulting in an interfacial dipole that reduces the effective work function. TDAE is a small molecule that exists in liquid form at room temperature and is unstable in air. The last property is highly undesirable in terms of application in devices, so there is a need for replacing TDAE with a more stable molecule. Very recently Bröker et al. investigated neutral methyl viologen (1,1'-dimethyl-1H,1'H-[4,4']bipyridinylidene, MV0) deposited on Au (111) using ultraviolet photoelectron spectroscopy (UPS). As a result of MVO-to-Au electron transfer, the work function of Au (111) was decreased from 5.50 to 3.30 eV. The energy levels of electron transport layers

\*Corresponding author. E-mail: fhli@ifm.liu.se.

- (1) Crispin, X.; Geskin, V.; Crispin, A.; Cornil, J.; Lazzaroni, R.; Salaneck, W. R.; Bredas, J. L. *J. Am. Chem. Soc.* **2002**, *124*, 8131.
- (2) Ishii, H.; Sugiyama, K.; Ito, E.; Seki, K. *Adv. Mater.* **1999**, *11*, 605.
- (3) Braun, S.; Salaneck, W. R.; Fahlman, M. *Adv. Mater.* **2009**, *21*, 1450.
- (4) Vazquez, H.; Flores, F.; Kahn, A. *Org. Electron.* **2007**, *8*, 241.

- (5) Heimel, G.; Romaner, L.; Zojer, E.; Brédas, J. L. *Acc. Chem. Res.* **2008**, *41*, 721.
- (6) Hino, S.; Umishita, K.; Iwasaki, K.; Tanaka, K.; Sato, T.; Yamabe, T.; Yoshizawa, K.; Okahara, K. *J. Phys. Chem. A* **1997**, *101*, 4346.
- (7) Jakobsson, F. L. E.; Crispin, X.; Lindell, L.; Kancierzewska, A.; Fahlman, M.; Salaneck, W. R.; Berggren, M. *Chem. Phys. Lett.* **2006**, *433*, 110.
- (8) Lindell, L.; Burquel, A.; Jakobsson, F. L. E.; Lemaire, V.; Berggren, M.; Lazzaroni, R.; Cornil, J.; Salaneck, W. R.; Crispin, X. *Chem. Mater.* **2006**, *18*, 4246.
- (9) Lindell, L.; Unge, M.; Osikowicz, W.; Stafstrom, S.; Salaneck, W. R.; Crispin, X.; de Jong, M. P. *Appl. Phys. Lett.* **2008**, *92*, 163302.
- (10) Osikowicz, W.; Crispin, X.; Tengstedt, C.; Lindell, L.; Kugler, T.; Salaneck, W. R. *Appl. Phys. Lett.* **2004**, *85*, 1616.

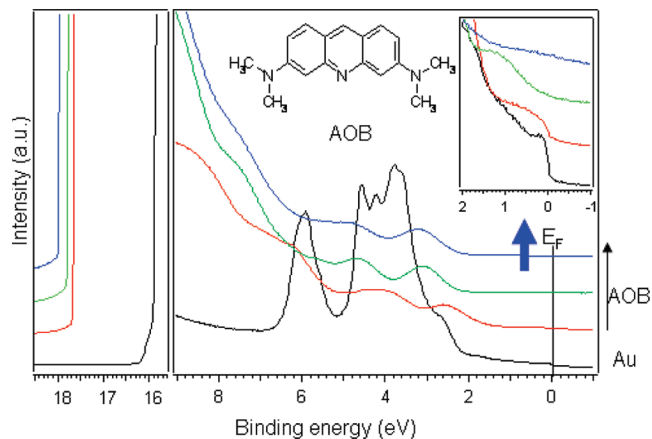


**Figure 1.** UPS spectra of sputter-cleaned Au (black line), one (sub) monolayer AOB on Au (red line), and two multilayer AOB thin films on Au (green line and blue line). Insets show molecular structure of AOB and the valence band spectra blown up from  $-1$  to  $2$  eV.

deposited on top of modified Au surfaces were shifted to higher binding energies compared to layers on pristine Au, and the electron injection barrier was reduced by  $0.80$  eV for tris(8-hydroxyquinoline)aluminum ( $\text{Alq}_3$ ) and by  $0.65$  eV for  $\text{C}_{60}$ .<sup>11</sup> Here, we present another air-stable donor acridine orange base (AOB, molecular structure is depicted in Figure 1) to modify the WF of polycrystalline Au. AOB can be an effective n-dopant for organic electron transport materials, as demonstrated for  $\text{C}_{60}$  thin films.<sup>12,13</sup> AOB has a number of advantages over TDAE as an electron donor, such as (i) being air stable, (ii) existing as a solid powder that can be vapor-deposited in vacuum, and (iii) being commercially less expensive, all of which makes AOB more appropriate for use in real device applications. In this paper, we study the energy level alignment at  $\text{C}_{60}/\text{Au}$ ,  $\text{AOB}/\text{Au}$  and  $\text{C}_{60}/\text{AOB}/\text{Au}$  interfaces in order to clarify if thin AOB sandwich layers can significantly lower the effective work function of gold, and if so, by which mechanism. We further test the validity of using Au molecularly modified by AOB as a low-work-function electrode in a set of polymer solar cells with  $\text{APFO3}:\text{PCBM}$ <sup>14</sup> as the active layer and discuss the general applicability of this approach using other high work function substrates.

### Experimental Section

For the chemical structures of AOB, we refer to Figure 1.  $\text{C}_{60}$  ( $>99.9\%$ , MER, Tucson) and AOB (Aldrich, dye content  $>75\%$ ) was purified twice and once by gradient sublimation in high vacuum before use. All organic thin films were prepared by thermal evaporation in situ in vacuum with a base pressure  $1 \times 10^{-8}$  mbar. Au substrates were sputter-cleaned with an argon gas until WF of Au reached  $5.1 \pm 0.1$  eV and no oxygen

and carbon signals were detected. The ultraviolet photoelectron spectroscopy (UPS) characterizations were carried out with monochromatized HeI radiation at  $21.2$  eV for every step of AOB or  $\text{C}_{60}$  deposition. The deposition process was additionally aided by X-ray photoelectron spectroscopy that was used to monitor the thickness of AOB or  $\text{C}_{60}$  overlayer from the attenuation of substrate core level signal. For AOB deposited on  $15$  nm  $\text{C}_{60}$ , the thickness of AOB was calculated using evaporation rate and evaporation time. Sandwich-structure devices were prepared by spin-coating first the hole injection polymer layer PEDOT:PSS ( $45$  nm, Bayer AG, EL grade) and then the blend active layer poly[(9,9-dioctylfluorenyl-2,7-diyl)-co-5,5-(4',7'-di-2-thienyl-2',1',3'-benzothiadiazole)] (APFO3):[6,6]-phenyl- $\text{C}_{61}$ -butyric acid methyl ester (PCBM) ( $50$ – $60$  or  $80$  nm) on a cleaned ITO-coated glass substrate, and finally vacuum-depositing  $2$  nm AOB/ $50$  nm Au or  $50$  nm Au as the electrodes. The samples were characterized using both high-intensity white-light illumination from a solar simulator AM1.5 ( $1000\text{Wm}^{-2}$ ) and Keithley 2400 source meter. Open circuit voltage and power conversion efficiency were derived from  $I$ – $V$  characteristics. All measurements were carried out in ambient atmosphere. Experimental details are described in ref 14.

### Results and Discussions

The energy-level alignment at interfaces between AOB and Au was investigated using UPS. Figure 1 shows the UPS spectra of sputter-cleaned Au, AOB (sub)monolayer and two AOB multilayer samples deposited in situ on Au at room temperature. Here it should be noted that we simply refer to more or less  $1$  nm AOB as a (sub)monolayer since at this range of thickness the AOB film is not able to fully cover the polycrystalline Au surface (large Au surface roughness due to sputtering by Ar and possible island growth). The WF is defined by the secondary electron cutoff in the left-hand-panel. When an AOB (sub)monolayer is vapor-deposited on the Au substrate, the WF of the Au substrate changes from  $5.2$  to  $3.5$  eV because of the formation of an interface dipole that downshifts the work function by  $1.7$  eV. With increasing AOB deposition, the WF of AOB thin films on Au substrates reaches a steady value  $3.3$  eV at full coverage of the Au surface indicating an interfacial dipole energy of  $1.9$  eV for the AOB/Au contact. To discover the origin of such a large shift in WF, we show a blow-up of the valence band spectra in the energy gap region in the inset of Figure 1. A broad feature located around  $1$  eV gradually appears upon the deposition of AOB until full coverage is reached (green spectrum). After further deposition resulting in thicker AOB multilayers, the intensity of this new peak becomes weaker and finally disappears, suggesting that it is only AOB molecules at the gold surface that contributes to this feature. We assign this new broad feature to the singly occupied molecular orbital (SOMO) of the  $\text{AOB}^+$  radical cation, which is characterized by the destabilization of the HOMO, similar to the case of  $\text{TDAE}^+$ .<sup>9</sup> AOB is a heterocyclic compound with  $n \rightarrow \pi^*$  transitions. Single electron release of lone pair ( $n$ ) electrons at the cyclic nitrogen atom incorporated into the  $\pi$ -system of AOB to Au leaves an  $\text{AOB}^+$  radical cation

- (11) Bröker, B.; Blum, R.-P.; Frisch, J.; Vollmer, A.; Hofmann, O. T.; Rieger, R.; Müllen, K.; Rabe, J. P.; Zojer, E.; Koch, N. *Appl. Phys. Lett.* **2008**, *93*, 243303.  
 (12) Harada, K.; Li, F.; Maennig, B.; Pfeiffer, M.; Leo, K. *Appl. Phys. Lett.* **2007**, *91*, 92118.  
 (13) Li, F.; Pfeiffer, M.; Werner, A.; Harada, K.; Leo, K.; Hayashi, N.; Seki, K.; Liu, X. J.; Dang, X. D. *J. Appl. Phys.* **2006**, *100*, 023716.  
 (14) Zhang, F. L.; Jespersen, K. G.; Björstrom, C.; Svensson, M.; Andersson, M. R.; Sundstrom, V.; Magnusson, K.; Moons, E.; Yartsev, A.; Inganäs, O. *Adv. Funct. Mater.* **2006**, *16*, 667.

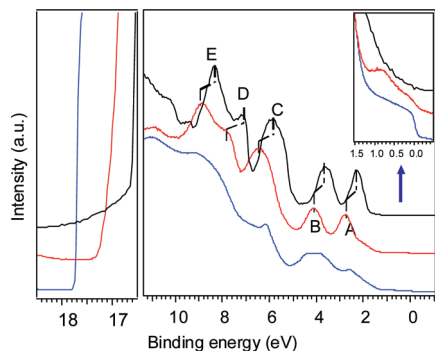


**Figure 2.** UPS spectra of one (sub)monolayer AOB on Au (blue line, work function is 3.5 eV), 3 nm  $C_{60}$  on AOB/Au (red line, work function is 4.2 eV), and 3 nm  $C_{60}$  on Au (black line, work function is 4.6 eV). Inset shows the valence band spectra blown up from  $-0.5$  to  $1.5$  eV.

that contributes to the photoelectron signal intensity. It is this electron transfer from AOB to the Au surface at the interface that together with the so-called push-back effect<sup>15</sup> creates the interfacial dipole of 1.9 eV at the AOB-Au interface at full coverage. This is analogous to the observed behavior for TDAE deposited on Au substrates.<sup>9</sup> Recently Hofmann et al. carried out a computational investigation of electron donors tetrathiafulvalene and viologen on coinage metal surfaces (Au, Ag, and Cu) using density functional theory based band-structure calculation. They predicted the work function of Au is reduced by up to 1.6 eV when Au surface is covered by viologen.<sup>16</sup> Their theoretical findings are in principle consistent with our UPS experimental results.

From the experimental UPS spectra depicted in Figure 1, the vertical ionization potential (IP) of AOB is  $5.4 \pm 0.1$  eV vs vacuum level. The electron affinity (EA) of AOB can be estimated to be roughly equal to 2.9 eV using the vertical IP and optical band gap, though note that such a procedure generally introduces large errors in the EA estimate.

Using organic semiconductor  $C_{60}$  as a model system for [6,6]-phenyl- $C_{61}$ -butyric acid methyl ester (PCBM), we probe the energetics at the AOB-modified gold cathode:  $C_{60}$ /AOB/Au. Figure 2 shows the UPS-derived valence band spectra of a (sub)monolayer of AOB on Au, a 3 nm  $C_{60}$  thin film deposited on AOB/Au, and a 3 nm  $C_{60}$  deposited on Au. The WF of an Au substrate with a (sub) monolayer of AOB is 3.5 eV (bottom spectrum in Figure 2). When 3 nm  $C_{60}$  is deposited on the AOB/Au substrate (middle spectrum in Figure 2), the WF changes to 4.2 eV and the valence band spectrum presents the typical five features (A–E) of  $C_{60}$ . For comparison, when a 3 nm pristine  $C_{60}$  film is directly deposited on sputter-cleaned Au (WF of 5.2 eV), the resulting WF is reduced to 4.6 eV (top spectrum in Figure 2). The interfacial dipole of 0.6 eV at the  $C_{60}$ /Au interface is mainly due to the “push back effect” at the clean Au surface that decreases the effective work function.<sup>15</sup> Compared to 3 nm  $C_{60}$  on Au, each of the five electronic features, A–E, of 3 nm  $C_{60}$  on

AOB/Au is shifted by  $\sim 0.5$  eV uniformly toward higher binding energy than for  $C_{60}$  on Au. An analogous shift attributed to charge transfer has been observed in the UPS spectrum of TDAE- $C_{60}$  complex.<sup>6</sup> Hence, the shift is an indication that electron transfer to  $C_{60}$  takes place at the interface between  $C_{60}$  and AOB/Au. Adding a thin AOB film between  $C_{60}$  and Au thus gives rise to a Fermi level shift away from the HOMO and toward LUMO of  $C_{60}$ . As a result, the barrier of electron injection into  $C_{60}$  is reduced. In addition, all five peaks are slightly broader than the corresponding ones in the black spectrum for 3 nm  $C_{60}$  on Au. This broadening also is present in the TDAE- $C_{60}$  spectrum because of the Jahn–Teller effect.<sup>6</sup> The peak involved with Jahn–Teller active  $h_g$  mode of  $C_{60}^-$  appears in the FTIR spectrum of mixed  $C_{60}$ :AOB thin films.<sup>17</sup> We hence assign the shift and broadening of the peaks in the UPS spectrum to electron transfer from AOB to  $C_{60}$  at the interface. Direct evidence of charge transfer at the interface is observed in the blow-up of the energy gap region in valence band spectra shown in the inset of Figure 2. Comparing the spectra of AOB/Au and  $C_{60}$ /Au, a new peak around 0.9 eV below Fermi level, assigned to  $C_{60}^-$ , is clearly visible in the spectrum of  $C_{60}$  on AOB/Au while there is no observable feature in the energy gap region of  $C_{60}$  on Au. The appearance of a new peak of similar binding energy has also been observed in the case of  $C_{60}$  doped with alkali metals<sup>18,19</sup> as well as for physisorbed  $C_{60}^-$ ,<sup>20</sup> supporting our assignment of the feature as resulting from negatively charged  $C_{60}$  molecules.

The UPS-derived energy level alignment diagrams for the  $C_{60}$ /Au interface and the  $C_{60}$ /AOB/Au interface are depicted in Figure 3a and b, respectively. The effective work function of the  $C_{60}$ /Au cathode is 4.6 eV according to the UPS results, i.e., electron injection into the next  $C_{60}$  layers is made from this rather deep level (Figure 3a). For the  $C_{60}$ /AOB/Au cathode (AOB (sub)monolayer), the interfacial dipole at the AOB/Au interface downshifts the WF to 3.5 eV and the interfacial dipole at the  $C_{60}$ /AOB interface upshifts the WF by 0.7 eV (the dipole here has its negative pole on the side of  $C_{60}$  due to an electron transfer from AOB to  $C_{60}$ ) giving a total vacuum level shift from Au to  $C_{60}$  of 1.0 eV for the  $C_{60}$ /AOB/Au contact (Figure 3b). Hence, the effective work function for electron injection into the next  $C_{60}$  layers beyond the interface is 4.2 eV, 0.4 eV lower than for the pure  $C_{60}$ /Au cathode. Therefore, the experimental results suggest that adding a thin AOB film should improve electron injection from Au contact into  $C_{60}$  film by downshifting the effective work function and by introducing n-doped  $C_{60}$  at the interface region. We stress again that one (sub)

(15) Osikowicz, W.; de Jong, M. P.; Braun, S.; Tengstedt, C.; Fahlman, M.; Salaneck, W. R. *Appl. Phys. Lett.* **2006**, *88*, 193504.

(16) Hofmann, O. T.; Rangger, G. M.; Zojer, E. *J. Phys. Chem. C* **2008**, *112*, 20357.

(17) Li, F. Novel dopants for n-type doping of electron transport materials: cationic dyes and their bases. PhD Thesis, Technische Universität Dresden, Dresden, Germany, 2005; p 87.

(18) Hino, S.; Matsumoto, K.; Hasegawa, S.; Iwasaki, K.; Yakushi, K.; Morikawa, T.; Takahashi, T.; Seki, K.; Kikuchi, K.; Suzuki, S.; Ikemoto, I.; Achiba, Y. *Phys. Rev. B* **1993**, *48*, 8418.

(19) Wertheim, G. K.; Buchanan, D. N. E. *Phys. Rev. B* **1993**, *47*, 12912.

(20) Jönsson, S. K. M.; Salaneck, W. R.; Fahlman, M. *J. Appl. Phys.* **2005**, *98*, 14901.

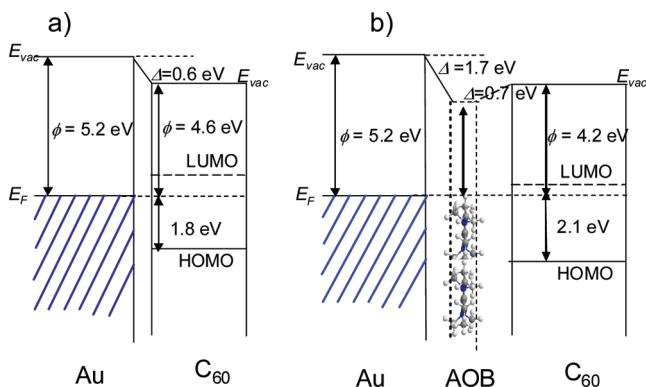


**Figure 3.** Energy-level alignment diagrams of bulk  $C_{60}$  thin film on (a) Au and (b) AOB/Au.

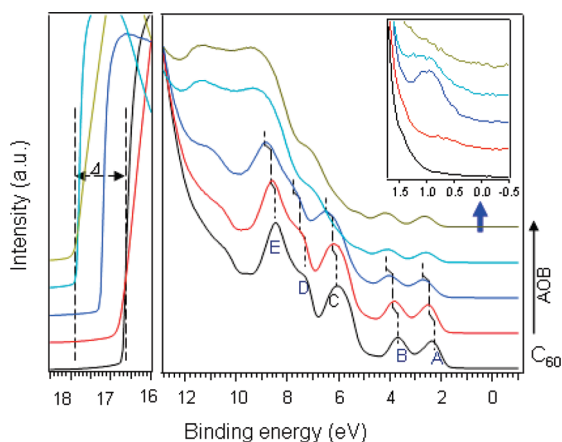


**Figure 4.** UPS spectra of 15 nm  $C_{60}$  thin film (bottom) and AOB thin films with various thicknesses (red for 2–4 Å, blue for about 9 Å, the top two for about 3 and 4 nm, respectively). Inset shows the valence band spectra blown up from –0.5 to 1.5 eV.

monolayer AOB does not fully cover the Au surface and the  $C_{60}$ /AOB/Au contact in Figure 3b is a complicated mixed interface. Figure 3b does not imply that an AOB molecule donates electrons to both Au and  $C_{60}$  at the same time.

The evolution of the WF and UPS-derived HOMO with increased coverage of  $C_{60}$  on AOB/Au is also investigated (see the Supporting Information). With the deposition of  $C_{60}$  on AOB/Au, the WF increases from 3.5 to 4.2 eV with increasing coverage. After the thickness of  $C_{60}$  reaches 3 nm, the WF of sample is independent of the thickness of  $C_{60}$  and kept at a constant of 4.2 eV. For the  $C_{60}$ /Au contact, the WF stabilizes already after only 1 nm  $C_{60}$  coverage, suggesting that some intermixing of AOB and  $C_{60}$  may occur.

Given the possible  $C_{60}$ -AOB intermixing, further experiments are needed to exclude the possibility of  $C_{60}$ /Au interactions affecting the interface energetics for thin AOB sandwich layers. AOB hence was deposited on 15 nm thick  $C_{60}$  films to study the AOB/ $C_{60}$  interface. The UPS spectrum of a pristine 15 nm thick  $C_{60}$  film on an Au substrate is depicted in Figure 4 (bottom spectrum). Upon AOB deposition, the WF decreases gradually from 4.6 eV ( $C_{60}$  on Au) and stabilizes at 3.3 eV, the same value

as for AOB/Au, which indicates that the positive integer charge transfer level of AOB is located at 3.3 eV.<sup>21</sup> Furthermore, when AOB is deposited on  $C_{60}$ , a new peak around 0.9 eV appears gradually and reaches a maximum intensity when  $C_{60}$  is covered by a (sub)monolayer AOB (blue spectrum), see inset of Figure 4. After further deposition resulting in AOB multilayers on  $C_{60}$ , the peak becomes weaker and weaker and finally disappears when  $C_{60}$  is covered by 4 nm AOB (top spectrum). The appearance of the new peak in the energy gap region indicates electron transfer from AOB to  $C_{60}$  as discussed earlier. For a (sub)monolayer AOB on  $C_{60}$  (blue spectrum), the valence features of underlying  $C_{60}$  layer are still clearly visible. The trends in terms of the shift and broadening of the peaks are quite similar to those in the spectrum of 3 nm  $C_{60}$  on (sub)monolayer AOB/Au (Figure 2), with the Fermi level moving away from the HOMO and toward the LUMO level of  $C_{60}$  at the AOB/ $C_{60}$  interface. With multilayer coverage of  $C_{60}$  surface by AOB, the valence features of  $C_{60}$  are suppressed by the ones of AOB and the peak corresponding to charge transfer disappears (Figure 4, inset), demonstrating that the charge transfer occurs at the AOB/ $C_{60}$  interface region. It is clear that the dipole-induced WF decrease to 3.3–3.5 eV occurs because of AOB-to- $C_{60}$  charge transfer and  $C_{60}$ -Au interactions hence can be discounted when determining the energetics of  $C_{60}$ /AOB/Au interfaces even for (sub)monolayer AOB films.

We aim to prove that conventional electrodes with high WF (Au, Ag, ITO, PEDOT:PSS, and so on) are able to potentially function as effective cathodes after molecular-modification by AOB. We prepared a set of polymer solar cells with 1–2 nm AOB/Au replacing LiF/Al as the cathode. The results for polymer solar cells with structure: ITO/PEDOT:PSS/APFO3:PCBM(1:4 wt %)/AOB/Au are summarized in Figure 5. For comparison, devices without AOB thin films: ITO/PEDOT:PSS/APFO3:PCBM(1:4 wt %)/Au were fabricated and shown in the same figure as well; 50–60 or 80 nm active layer (APFO3:PCBM) are sandwiched between transparent anode and cathode. As is commonly known, poor matching between the cathode WF and PCBM LUMO will lead to reduced open circuit voltage ( $V_{oc}$ ) in the devices. The devices with the AOB-modified Au cathode have an open circuit voltage of nearly 1 V, which is similar with otherwise identical devices using LiF/Al as the cathode.<sup>14</sup> In addition, devices with AOB/Au have comparable power conversion efficiency (PCE) to devices with LiF/Al cathodes<sup>14</sup> even though AOB/Au is a poor reflection electrode. However, devices with Au as a cathode behave poorly in terms of  $V_{oc}$  and PCE because of the high WF of Au and thus poor matching to the PCBM LUMO (Figure 5). We can conclude that the AOB-modified Au electrode is an efficient low-work-function contact, as predicted by the UPS results.

We expect that AOB-modified metal electrodes as low-work-function contacts should be of general use. For instance, Singh et al. recently have pointed out that use of higher-work-function metal electrodes, viz., Cr, Au,

(21) Tengstedt, C.; Osikowicz, W.; Salaneck, W. R.; Parker, I. D.; Hsu, C.-H.; Fahlman, M. *Appl. Phys. Lett.* **2006**, *88*, 053502.

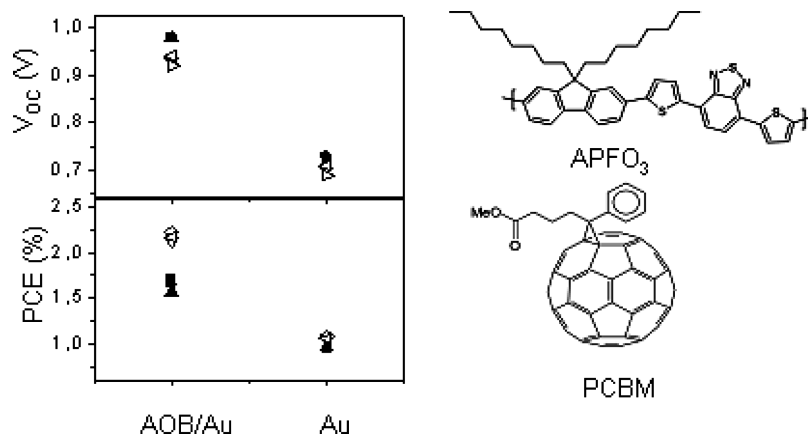


**Figure 5.** Open circuit voltage and power conversion efficiency of ITO/PEDOT:PSS/APFO<sub>3</sub>:PCBM(1:4 wt %)/cathode (Au or AOB/Au). Open symbols for the devices with 50–60 nm active layer and filled symbols for the devices with 80 nm active layer.

etc., in organic field effect transistors (OFETs) leads to slightly reduced mobility presumably because of large contact resistance.<sup>22</sup> In their field effect transistors of C<sub>60</sub> thin film prepared by hot wall epitaxy, the mobility can reach 0.4–1 cm<sup>2</sup>/V s when LiF/Al is used as source and drain contacts.<sup>23</sup> In analogy with our solar cells results, AOB/Au should then be expected to be a candidate for promising source/drain electrodes in n-type OFET. In fact, an Ohmic contact is formed between AOB-doped-C<sub>60</sub> thin film and Au as shown by field effect measurements.<sup>12,13</sup> The WF of other electrodes such as Ag, ITO, La<sub>0.7</sub>Sr<sub>0.3</sub>MnO<sub>3</sub>, and even PEDOT:PSS can be also effectively decreased by adsorbing an AOB thin film because of electron transfer from AOB to the substrates, thanks to the low positive pinning energy of AOB (3.3 eV). The AOB-adsorbate approach enables stable metal electrodes with high WF to be used as cathodes while avoiding many of the problems related to the use of TDAE.

### Conclusion

The WF of Au can be decreased significantly by adsorbing an AOB thin film. When a (sub)monolayer AOB is deposited on sputter-cleaned Au, the WF of the substrate changes from 5.2 to 3.5 eV. At complete cover-

age of the Au surface, the WF is further reduced to 3.3 eV. Dipole formation at interface is achieved by electron transfer from AOB to Au at the interface. When a (sub) monolayer of AOB is inserted between Au and C<sub>60</sub> thin film, the barrier of electron injection is decreased by  $0.4 \pm 0.1$  eV as compared to an Au–C<sub>60</sub> interface without AOB. Electron transfer from AOB to C<sub>60</sub> is observed. Polymer solar cells with AOB/Au as a cathode have a similar Voc and comparable PCE with devices using LiF/Al as a cathode, demonstrating that the AOB-modified gold electrode is an efficient low-work-function contact. Given the low positive pinning energy of 3.3 eV for AOB, we expect that other conventional high-work-function materials (Ag, ITO, La<sub>0.7</sub>Sr<sub>0.3</sub>MnO<sub>3</sub> and even PEDOT:PSS) can be modified by AOB as effectively as Au.

**Acknowledgment.** This work was carried out within the EU Integrated Project OFSPIN (EU-FP6-STREP). We gratefully acknowledge organic solar cells group at Institut für Angewandte photophysik, Technische Universität Dresden, Germany, for supplying AOB purified once and C<sub>60</sub> purified twice. F.L. thanks Dr. Wojciech Osikowicz for discussion in terms of C<sub>60</sub>. In general, the Surface Physics and Chemistry division is supported by the Swedish Research Council (project grant and Linneus center) and the Knut and Alice Wallenberg Foundation.

**Supporting Information Available:** Evolution of the work function and HOMO with the deposition of C<sub>60</sub> on Au and C<sub>60</sub> on AOB/Au (PDF). This material is available free of charge via the Internet at the <http://pubs.acs.org>.

- (22) Singh, T. B.; Marjanovic, N.; Stadler, P.; Auinger, M.; Matt, G. J.; Gunes, S.; Sariciftci, N. S.; Schwodiauer, R.; Bauer, S. *J. Appl. Phys.* **2005**, *97*, 083714.  
 (23) Singh, T. B.; Marjanovic, N.; Matt, G. J.; Gunes, S.; Sariciftci, N. S.; Ramil, A. M.; Andreev, A.; Sitter, H.; Schwodiauer, R.; Bauer, S. *Org. Electron.* **2005**, *6*, 105.